A Network-Based Method to Analyze EMI Events of On-Board Signaling System in Railway

Meng Li [1], Yinghong Wen [1,2,*], Guodong Wang [1,2], Dan Zhang [1,2,*] and Jinbao Zhang [1,2]

[1] Electromagnetic Compatibility Research Institution, School of Electronic and Information Engineering, Beijing Jiaotong University, Beijing 100044, China; mengli@bjtu.edu.cn (M.L.); gdwang@bjtu.edu.cn (G.W.); jbzhang@bjtu.edu.cn (J.Z.)

[2] Beijing Engineering Research Center of EMC and GNSS Technology for Rail Transportation, Beijing 100044, China

[*] Correspondence: yhwen@bjtu.edu.cn (Y.W.); zhang.dan@bjtu.edu.cn (D.Z.)

Abstract: The On-board Train Control System (OTCS) plays an important role in the real-time operation of the electric multiple units (EMU) in high-speed railway. The EMU is a complex system made up of various electrical and electronic equipment, so the interactions of the electromagnetic (EM) environment and OTCS are difficult to study, which leads to more challenges to analyze EM interference (EMI) events at the system level. To overcome this difficulty, this paper proposes the thought of a graph model to solve the problem. First, a framework is proposed to more clearly reflect the relationship between the EMC (Electromagnetic Compatibility) problem and network through a comparison with them. Second, a network theory-based model is presented to express the EMC elements for the OTCS in EMU. It decomposes the OTCS and EMU with EMC elements into edges and nodes of the network, which parameters are defined corresponding to EM sources, sensitive equipment, and coupling paths. Thus, each part could be modeled separately or together by calculation, simulation, or measurement, respectively, and the EMC problem could be represented by the paths from origin to destination in the network. Moreover, the modeling process was elucidated by the specific cases in OTCS and the validity of the proposed approach was verified by calculation and measurement results in the case study.

Keywords: EMC; system-level analysis; on-board train control system; EM disturbance; network model; EM interactions; measurement and simulation verification

1. Introduction

The electric multiple units (EMU) are becoming increasingly advanced and intelligent with the new technology applied in the world railway system, such as the new types of CR (Fuxing in China Railway) series in China in the last years. Risks from electromagnetic (EM) disturbance to the On-board Train Control System (OTCS) has been spotlighted and investigated in the railway industry [1–5], because it may cause serious fault or failure when the electric and electronic parts are subjected to them. To ensure the safe operation of the EMU, system-level EMC analysis of OTCS is essential and it is regarded as one tough work with the following features. The OTCS is a complex system that the subsystems and components are distributed throughout the EMU. During the continuous movement of EMU, interactions between high power sources (mainly from the traction power supply and drive system) and safety-critical systems (OTCS) will occur, and it is a different EM environment from other industries. Thus, EM modeling and test for every EMC problem of subsystem require large-scale computation and massive measurement. However, the traditional solutions facing such a system-level assessment are limited.

Components and equipment in OTCS are required to fulfill the requirements of EMC regulations such as the IEC 62236 series before installation and application [6]. Therefore, there are no systems in OTCS that have not been qualified for EMC. Despite these numerous tests, the OTCS is still broke down possibly due to the special EM environment in high-speed railway. There is a disparity that leads to the EMC problems in OTCS between the tested EM environment in the laboratory and actual on-site conditions. In general, even if some measures have been taken for the EM interference problem of a particular subsystem, there may cause another problem in other subsystems in the limited space. To prevent EM disturbance generated by the traction power supply and drive system in EMU from interfering with the performance of OTCS, considerable research work has been done on this issue by manufacturers, researchers, and operators related to the railway domain.

There are numerous sources of EM disturbances in the high-speed railway system. Through deep investigation and measurement of the EM environment in railway, it can be found that the sources derive from two major parts of the EMU. One is the traction power supply system and the other is the traction propulsion system [7–13]. The former mainly comes from the pantograph arcing at the offline moment from the pantograph and the contact wire due to the inevitable vibration. Reference [7] presented a measurement to investigate EM interference phenomena in pantograph arcing and the results showed a significant difference between the pantograph going up and down. Additionally, a foundation of the pantograph arcing process was formed by experimental analyses of pantograph arcing phenomena with the AC supply [8]. Because of the difficulty in calculating the radiated disturbance from pantograph arcing, a method that combines numerical modeling and reverberation chamber measurements was proposed in Reference [9]. Moreover, Reference [10] showed the radiated emission of a high-speed railway system by modeling and experimental measurements based on the multi-conductor transmission line theory. The latter parts including the transformer, converters, and motors export most of the sources with transient disturbance. References [11,12] discussed the EM sources in the traction system by practical measurement. For the study and prediction of the EMC problems in the propulsion system, the high-frequency model containing converter and traction motor is developed in Reference [13].

On the other hand, concerning the EM interference (EMI) problems and equipment susceptibility of OTCS, most of the subsystems had been studied in different ways such as the GSM-R (Global System for Mobile Communications-Railway) [14,15], balise transmission module [5,16], track circuits [17,18], and cables [19]. Various solutions have been attempted to improve the OTCS EMC according to the interactions between the sources and equipment as mentioned above. Nevertheless, there is no detailed and distinct methodology framework on how to assess the whole system due to the complex couplings, huge scale computation, and massive test data. It is not easy to get a system-level view of the OTCS EMC, because any change in every part may lead to a new procedure of the simulation or measurement. This implies that a more powerful and clear method is needed to optimize work and judgment for OTCS EMC in railway engineering.

To date, there are primarily two means to study EMC problems in a complicated system. One is the lumped parameters equivalent circuits [20] and the other is transfer functions such as EM topology (EMT) [21]. Each of them has its advantages and disadvantages. Unlike the limitation in low-frequency range in the former one, the EMT method could decompose the complex system into multi-zones based on the shielding layer, and transfer functions could be adopted to describe the propagations by conduction and radiation. However, the accuracy transfer functions are not easy to obtain and the interactions between internal and external areas cannot be ignored sometimes. Therefore, we need to build a methodology for assessing the EMC of the whole OTCS, which may make engineers have the best understanding to have a global view.

In this work, we introduced a method based on network theory [22] to combine the tube and junction idea in EMT according to relevant electrical and EMC properties of the subsystems. A topological network is proposed with the edges and nodes to describe the interaction between the EM environment and the OTCS. The coupling and real connection between the sources and components

are described in OTCS. The description and definition of the parameters for elements in the constructed model of OTCS are explained. In Section 2, a novel EMC network framework and method are presented. Section 3 explains the network model of the OTCS in detail. In Section 4, the real case study for the subsystem from OTCS is implemented to verify the effectiveness of the proposed approach. Section 5 presents the conclusion.

2. Network-Based Modeling Framework and Method

2.1. Problems Description

The idea for the method presented in this paper was derived from a similar expression used in system engineering. The EMC problem of the system refers to the process in which EM disturbance sources (internal and external) affect the normal operation of the electrical and electronic functions of the corresponding parts through the transmission coupling relationship within the system. According to this description, it can be defined as:

$$D_{EMC} = (S, C, T, F) \tag{1}$$

where D_{EMC} denotes a definition function, S is the EM disturbance source in the specific EM environment, C represents the coupling path, and T is the equipment in the system. F denotes the function of the equipment or the system. Thus, the representation of EMC issues is very similar to the network as shown in Figure 1, where the left part is the description of the EMC problem including sources, coupling, and OTCS equipment in EMU. The right part is made up of the nodes and edges with different meanings of EMC elements.
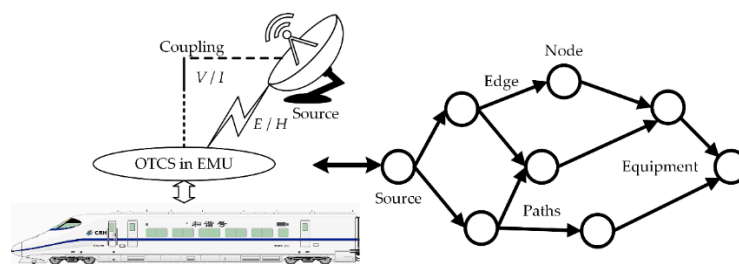

Figure 1. An analogy between the EMC problem and network.

According to the definition in Equation (1), the EMC problem is a network structure composed of different EMI events as shown in the upper of Figure 2. So, it can be regarded as a network structure formed by nodes and edges. In Figure 2, sources 1 and 2 (node v_1 and v_2) affect equipment 11 and 12 (node v_{11} and v_{12}) through two different paths, which represent different EMI events. Each node can represent the elements of EMC issues, such as EM disturbance sources and sensitive equipment. The edge indicates the propagation path that an EM disturbance source affects the target equipment through different coupling ways, such as the conduction and radiation. Each path from the source to the device can be represented as an EMI event. However, all of the EMI events will not occur at the same time due to different scenarios. If every EMI event of the system can be expressed through a network, it will be helpful in the EMC analysis at the design, verification, and application phases.
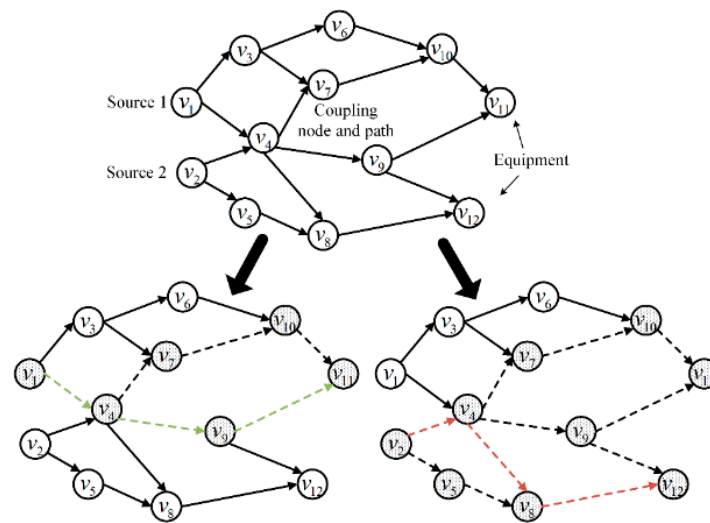
Figure 2. Different paths represent different electromagnetic interference (EMI) events in the EMC network. Path v_1 to v_{11} with a green line and path v_2 to v_{12} with a red line are two different EMI events.

2.2. EM Interactions between EMU and OTCS

For the EM environment in high-speed railway, different coupling manners are connecting the EM disturbance sources of the EMU and various parts of the OTCS equipment. The relations between the source in EMU and the equipment at the dispersed position are shown in Figure 3 and various EM couplings make the interactions extremely complicated. In general, there are two types of EM coupling, namely, conductive coupling and radiation coupling. The former includes conductive direct coupling and capacitive and inductive coupling. The latter contains antenna coupling, field line coupling, and cable coupling. Different sources can affect the target devices through the aforementioned coupling methods.
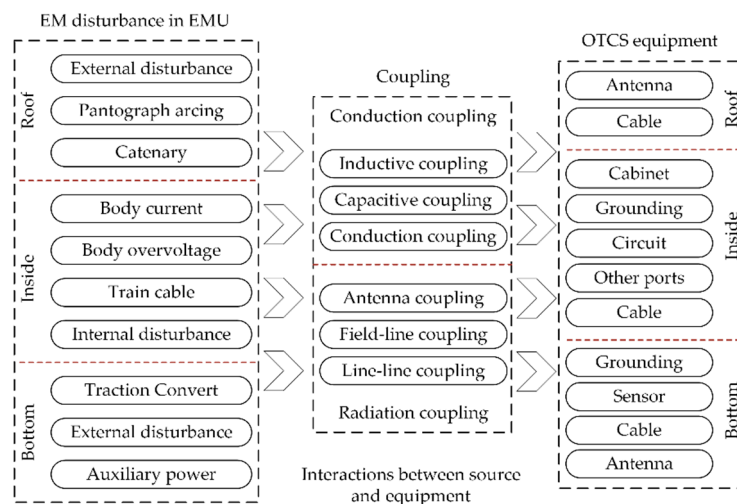

Figure 3. The EM interactions between electric multiple units (EMU) and on-board train control system (OTCS).

As shown in Figure 3, the EMU can be divided into the roof, interior, and bottom in space. Correspondingly, OTCS equipment is also distributed in the above three spaces, such as cables, antennas, cabinets, grounding, and sensors. Therefore, each EMI event corresponds to an interactive relationship in the figure. Thus, all events will become a complex network of connections. It will be helpful to analyze the OTCS EMC problems if all the interactions are transformed into the form of the network.

2.3. Framework of the EMC Network Model

The framework of the EMC network model is composed of two parts with a pink and blue dashed box, as shown in Figure 4. In the first part, the EMC network is proposed based on engineering and historical cases. Due to the complexity of the disturbance source and coupling mechanism, we have to investigate all possible situations under consideration. Thus, it is necessary to have comprehensive research on the characteristics of the disturbance such as location, frequency, types of coupling, and so on. In the second part, to analyze the EMI events, the structure and function of the OTCS should be known especially the connection and spatial relationship between the OTCS and EMU. Moreover, the modeling process is consistent with the interaction between the EM environment and system structure. The final EMC network model is based on the modeling process of this framework and the model consists well with the principle of the EMI event, i.e., the disturbance generated in the EM environment propagates in EMU and ultimately interferes with the OTCS in high-speed railway. However, the network model is only an auxiliary methodology that can help us to make the EMC analysis of the system more comprehensive. The study of each EMI event still relies on traditional EMC analysis methods, and it will be explained in the case study. In the following parts, the model is named the EN model for simplicity.
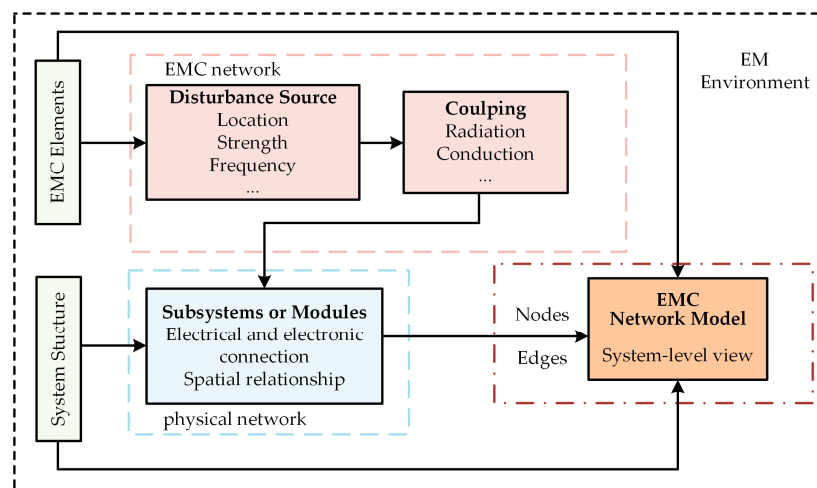

Figure 4. The framework of the EMC network model.

2.4. Approach of the Network Modeling

In this subsection, we aim to introduce the step-by-step approach and definitions applied in the EN model. The model construction is divided into several parts, including the definition and representation of the node, the definition and form of the edge, the model expression and simplification, and the procedure. Detailed descriptions are as follows:

1. The definition and representation of the node

The node is the basic unit of the network. It can represent the EMC elements and sensitive components in the target system. In other words, each node in the EN model, which has a consistent one-to-one match with the EMC elements and system functional structure, has a specific function and meaning. Thus, the attributes or characteristic parameters of the nodes can be obtained through calculation, simulation, or measurements, such as the amplitude, frequency, transfer function, and the module function. Based on the above definition, the node form can be determined in Table 1.

Table 1. The form of the node.

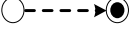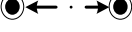| No.	Node	Form	EMC Elements
1	Disturbance node	○	Radiation source
2	Disturbance node	◉	Conduction source
3	Virtual node [1]	○	Radiation coupling
4	Virtual node	●	Conduction coupling
5	Module node	◉	Equipment
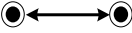
[1] The connections between disturbance and equipment.

There are two kinds of EM disturbance nodes in the running scenario of the high-speed railway. One is the radiated disturbance node and the other is the conducted disturbance node. The attributes of the source node can be represented by waveforms in standards or the parameters measured on-site. Besides, two virtual nodes are designed, which are the radiation and conduction coupling nodes. There are two advantages, on the one hand, the virtual node can be used to determine the coupling relationship between the disturbance source and the module nodes. On the other hand, it can reduce the complexity of the network by reducing the cross among the connection edges from the disturbance nodes to the module nodes.

2. The definition and form of the edge

Considering the coupling process of the EM disturbance in the EMC network domain, the connection relationship between the disturbance source and equipment is divided into two types, namely, the conduction and radiation coupling connections correspond to the coupling nodes in Table 1. Additionally, to address the connection in the system structure network domain, such as signal connection and physical connection, the form of the edge are designed in Table 2.

Table 2. The form of the edge.

Edge	Form	Explanation
Physical connection	◉◄────►◉	Contact by metal (ground)
Coupling connection a [1]	●────►◉	Conduction coupling
Coupling connection b [2]	○----►◉	Radiation coupling
Signal connection	◉◄─ · ─►◉	Wire transmission (unidirectional or bidirectional)
	◉◄----►◉	Wireless transmission

[1] The edge between the source and coupling nodes are the same with coupling connection. [2] Field-line coupling and inductive or capacitive coupling (crosstalk) are classified as this form for simplicity.

3. The model simplification and expression

Based on the definition of the node and edge in the EN model, if the results of the network achieve an acceptable level, the process is stopped and the model is analyzed in the next step. Otherwise, the model should be simplified by several times until there are no repetition and conflict between the nodes and edges. After the work above, the expression can be given with the format as:

$$
\begin{aligned}
EN \ &= G(V, E, A_v, A_e) \\
&= \begin{cases}
A_v = \{A_v(1), A_v(2), \cdots, A_v(n), \cdots, A_v(N)\}, n = 1, 2, \ldots, N \\
A_e = \{A_e(1), A_e(2), \cdots A_e(m), \cdots, A_v(M)\}, m = 1, 2, \ldots, M \\
\qquad v_i, v_j \in V, i \leq N, e_{ij} \in E, j \leq N
\end{cases}
\end{aligned}
\tag{2}
$$

where *EN* denotes the EN model; A_v and A_e are the attribute function for the node and edge separately, thus A_v and A_e can be represented by many forms such as simulation model, transfer function, and so on; *V* and *E* denote the sets of the nodes and edges; and *N* is the node number in the EN model.

4. Procedure

The overall procedure has the following five phases according to the preliminary above:

(1)   Basic information and materials to build the EN model are obtained from the system structure, documents, historical cases, expert experience, on-site measurement, and so on.
(2)   The nodes in the EMC domain and system structure domain are achieved and the properties are waiting for the decision by proper method.
(3)   According to the actual spatial location and connection relationship, the edges between the nodes are determined by the definition in Table 2.
(4)   The preliminary EN model will be adjusting, merging, and deleting nodes and edges for simplification. Then, the attribute function of the nodes and edges could be got by calculations, simulations, and measurements on the basis of their properties.
(5)   Repeat the steps above, and the final EN model is ready for application after optimization. Each path in the model can present a specific EMI event.

After that, the EMC problems of the target system are presented via a network based on the EN model.

3. EN Model of the OTCS

3.1. Traction System and the OTCS in EMU

The OTCS equipment is one of the important technical equipment to ensure the safe operation of the EMU in high-speed railway. The EMC problem in OTCS is mainly caused by the traction system in EMU, so the traction system and OTCS are first analyzed to obtain the information and materials and how to model.

3.1.1. Traction System

The traction system of the EMU consisted of the pantograph, high-voltage cable, traction transformer, traction converter, auxiliary power unit, traction motors, and ground device as shown in Figure 5. From the physical and electrical structure, it can be known that most of the devices and components of the traction system are concentrated on the top and bottom space of the EMU, except the pantograph on the roof. The electric energy is obtained through sliding on the contact wire of the catenary by the pantograph, and the motors propel the EMU in the traction drive system. As the conclusions in References [4,8], pantograph arcing is one of the sources in EMU.
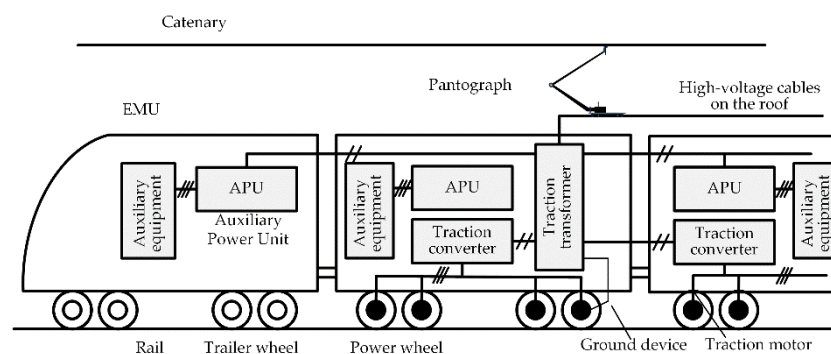

Figure 5. Structure diagram of the traction power and drive system of EMU.

There are three main channels for EM disturbances from the outside of the train to enter the inside of it: (1) radiation coupling by antennas on the roof and bottom of the vehicle, (2) direct radiation coupling in the body space, (3) conduction coupling related to the channel of "pantograph—traction transformer—traction converter—power line—ground device". However, EM disturbances from the inside of the train are more complex, especially the auxiliary circuits (auxiliary converters, batteries, and battery chargers, etc.), air conditioning, traction converters, and traction motors make the coupling complicated.

3.1.2. OTCS Equipment

The core function of the OTCS equipment is to supervise the speed of EMU in real-time and automatically control the braking system to prevent the train from over-speeding. A brief introduction of the CTCS-3 (Chinese Train Control System Level 3) level OTCS is given as an example below [23,24].

The subsystems and devices of the OTCS equipment cooperate with the wayside equipment to achieve real-time control. Figure 6 shows the structure diagram and locations of the OTCS, the main functions and features of the equipment are as follows:
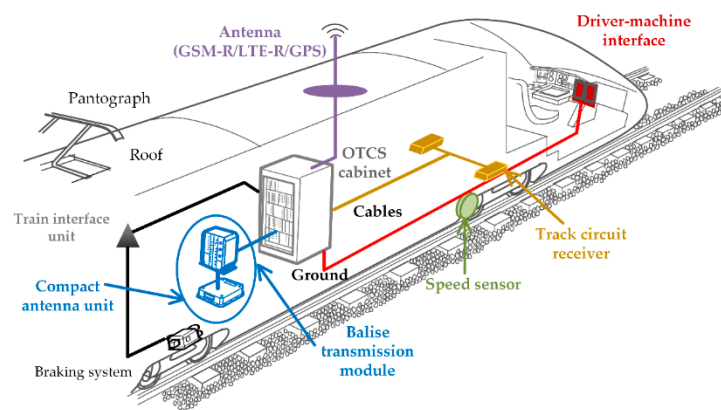

Figure 6. Structure diagram of the on-board train control system and layout.

- The roof of the EMU

The location and line data in the movement authority (MA) are sent and received by the antenna on the roof of the EMU between the OTCS and the wayside equipment via wireless communication. GSM-R is the most widely used and LTE-R (Long-Term Evolution for Railway) will be applied in the future.

- The bottom of the EMU

The speed sensor is used to acquire the speed and the over-speed protection is realized by the speed and distance processing unit (SDU) in OTCS with the acceleration data from the radar. The parts of the MA information from the track circuit and balise are acquired by the track circuit receiver (TCR) and compact antenna unit (CAU) in the balise transmission module (BTM). BTM can also calculate and calibrate the location in real-time.

- The insides of the EMU

The driver-machine interface (DMI) is used to show the interaction information to the driver and the driver can execute some instructions through DMI to control the EMU. The train interface unit (TIU) is used to provide an interface between the train and OTCS. The kernel of the OTCS and BTM are installed in the ATP cabinet with power and ground connection with the EMU.

3.2. EN Model of the OTCS

Considering the symmetry of the EMU, it takes 4-car of the 8-car EMU to model the OTCS for simplicity. Because there are two OTCS and traction systems in an 8-car EMU for redundancy. According to the procedure in Section 2, the nodes were deleted and merged based on the statistical data, expert knowledge, and literature. Then, the 26 nodes of the EN model are extracted and shown in Table 3 based on the structure in Figures 5 and 6.

Table 3. The nodes of the OTCS in the EN model.

Node	Node Description	Form	Node	Node Description	Form
v_1	External disturbance on the roof	⊖	v_{14}	Radiation coupling	○
v_2	Pantograph arcing (radiation)	○	v_{15}	DMI	◉
v_3	Pantograph arcing (conduction)	◉	v_{16}	Cable Between DMI and cabinet	◉
v_4	Traction system (high voltage cable)	◉	v_{17}	Antennas (GSM-R/LTE-R/GPS)	◉
v_5	Auxiliary power (power cables)	○	v_{18}	Cables in OTCS (I/O)	◉
v_6	Internal disturbance (insides of the EMU)	○	v_{19}	BTM	◉
v_7	Traction system (main circuit)	○	v_{20}	Cabinet (Kernel in OTCS)	◉
v_8	Auxiliary power (conduction)	⊖	v_{21}	Ground device	◉
v_9	Auxiliary power (radiation)	○	v_{22}	Speed sensor	◉
v_{10}	External disturbance at bottom	○	v_{23}	TCR	◉
v_{11}	Conduction coupling (Virtual node)	●	v_{24}	Antenna (CAU)	◉
v_{12}	Radiation coupling (Virtual node)	○	v_{25}	Cable in BTM and CAU	◉
v_{13}	Radiation coupling (Virtual node)	○	v_{26}	Radio Transmission Module	◉

Based on Table 3, we accomplished the EN model of the OTCS, which is described in Figure 7. There are four areas in the model and most of the connections are concentrated on the top and bottom areas. For the EMI events research, specific data, simulation model, and measurement will be presented and analyzed for each relevant element of the nodes and edges in Figure 7. However, it seems to be a difficult task for acquiring all of the possible paths in the model once time. The EN model of the OTCS will be updated based on the reports and research activities in the authority organization if a new EMI event occurs.
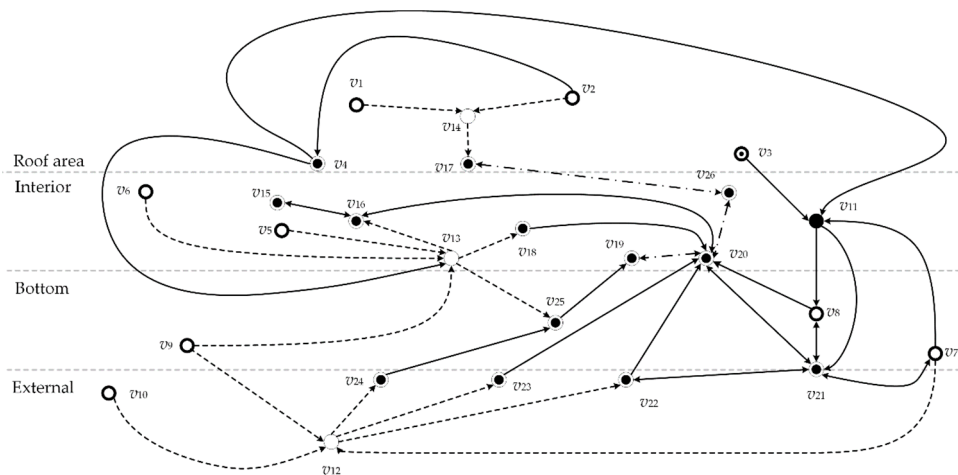

Figure 7. The EN model of the OTCS with an actual location in EMU.

4. Case Study

Section 3 has constructed the EN model of the OTCS to have a system-level view of the EMC topic. If certain properties of the nodes and edges can be found to analyze the paths from the on-site reports, the model can be used to resolve the new EMI event with the updated paths.

4.1. Paths Description

For the application of the EN model introduced in Sections 2 and 3, this section contains the actual cases of specific EMI events involving the disturbance and coupling. The content of the cases is presented in the subsequent sections. Figure 8 illustrates the paths with red and green lines concerning the interaction paths between the source and equipment.
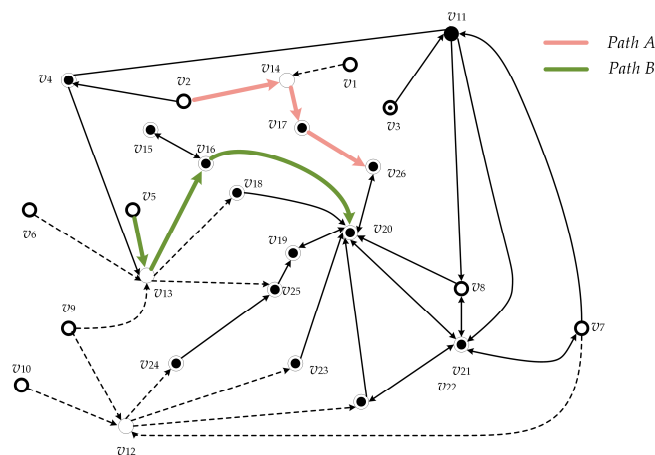

Figure 8. The case paths of the EMI events in EN model.

The LTE-R (LTE for railway) communications technology will be applied in the future and it has experimented with test lines by the railway group in China. The applicability of LTE-R in the 450 MHz frequency band should be considered according to the existing spectrum resource distribution in China. The transient radiated electric field from the pantograph arcing will have a potential impact on the performance of LTE-R at 450 MHz operation frequency [25]. The path of this case is the red line in Figure 8.

DMI (Driver-machine Interface unit) displays the information of control order, equipment status, and driving strategies of the train, as well as the fault information to the driver. It is located in the driver room connecting the kernel in OTCS by long cables. So, it could be influenced by the interaction between cables especially the nearby power lines in EMU. The path of this case is the green line in Figure 8.

Therefore, to verify the proposed modeling method for EMC in OTCS, these paths are used as practical examples in this study.

4.2. Paths in the Model

Although the explanation of the nodes can be found in Table 3, the reason for the events is still not investigated in detail. Here, we try to give the basic information and the attributions of the nodes and edges.

Figure 9 gives the path of the EMI event in case A. As we discussed above, v_2 is the disturbance from the pantograph arcing and v_{14} is the virtual coupling node of radiation. v_{17} is the antenna of the LTE-R and v_{26} is the function part. Then, the three edges are $e_{2\text{-}14}$, $e_{14\text{-}17}$, and $e_{17\text{-}26}$ correspondingly. In other words, for radiation coupling represented by v_{14}, the pantograph arcing in v_2 will be received at v_{17} and the influence on v_{26} can be reflected in an index of its function. It should be noted that not all of the attributions of the nodes and edges have specific values. Some of them indicate the deterministic

value for existence. In path A, $A_{e2\text{-}14}$ A_{v14}, and $A_{e17\text{-}26}$ are assigned with the deterministic value of 1. It indicates the path that happened in this scenario. On the contrary, A_{v2}, $A_{e14\text{-}17}$, and A_{v26} will be represented by measurement and simulation. In this case, A_{v17} is the measurement results from the receiving antenna, and A_{v26} can be considered as a result output module with a specific index by simulation.
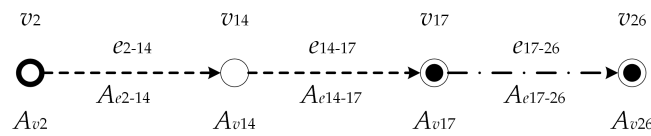

Figure 9. The path of case A.

Figure 10 gives the path of the EMI event in case B. v_5 is the disturbance from power lines in the auxiliary power and v_{13} is the virtual coupling node of cable coupling. v_{16} is the cable between the DMI device and the kernel v_{20} in OTCS. Then, the three edges are $e_{5\text{-}13}$, $e_{13\text{-}16}$, and $e_{16\text{-}20}$ correspondingly. The path has the following scene meaning, for cable coupling represented by v_{13}, the disturbance in power line in v_5 will be received by v_{16} and the influence on v_{20} can be reflected on the device v_{15}. If the signal cannot be received within a certain time, the DMI v_{15} will display a "communication interruption error". At this time, the v_{20} would give the emergency brake control order to the EMU leading to temporary parking. In this path, $A_{e5\text{-}13}$, $A_{e16\text{-}20}$, and A_{v13} are assigned with the deterministic value of 1. It indicates the path that happened in this scenario. A_{v5}, A_{v16}, and $A_{e13\text{-}16}$ will be represented by simulation and measurement. A_{v20} is the signal results at the cable terminal.
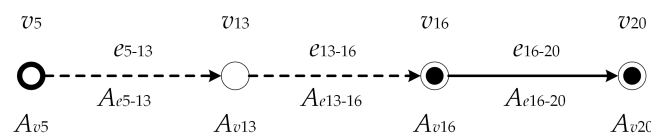

Figure 10. The path of case B.

4.3. Analysis and Discussion

4.3.1. Path A

1. A_{v2} of the node v_2

The pantograph arcing is selected as the attribute of A_{v2}. To obtain the actual waveform of the pantograph arcing during the operation of the EMU, a measuring probe is installed at the position of the train roof (see Figure 11a). As shown in the figure, the horizontal distance between the pantograph and the measurement antenna is 2.5 m and the antenna is 0.4 m in height above the roof. A coaxial cable is fixed on the outside of the train for connecting the instrument temporarily. The receiver and oscilloscope are set inside of the train under the control of the computer for data collection.

The single waveform of the EM disturbance from the pantograph arcing that is measured on-site is shown in Figure 11b. The duration of the single discharge is within 1 μs and the rise time is at nanoseconds (ns) level. However, the length of a symbol is around tens of μs in the communication system, i.e., the length of a symbol is about 72 μs in FDD-LTE (Long-Term Evolution Frequency-Division Duplex) with OFDM (Orthogonal Frequency-Division Multiplexing). Thus, the single waveform cannot cover the useful signals completely. It should be noted that most of the pantograph arcing from the off-line discharge is not a single pulse signal. There will be multiple arcing phenomena while the off-line between pantograph and catenary occur by sliding contact. The reason is that the off-line is continuous until the displacement difference between them is no longer zero. Therefore, it is assumed that the pantograph arcing disturbance is composed of multiple independent pulse signals like the waveform in Figure 11b. To get the time interval (TI) of the pulse, statistical analysis of the TI in

50 sets of scanning results is done based on the Weibull distribution. Thus, the continuous disturbance composed of the waveform in Figure 11b with about 0.17 ms TI is regarded as the attribute of v_2.
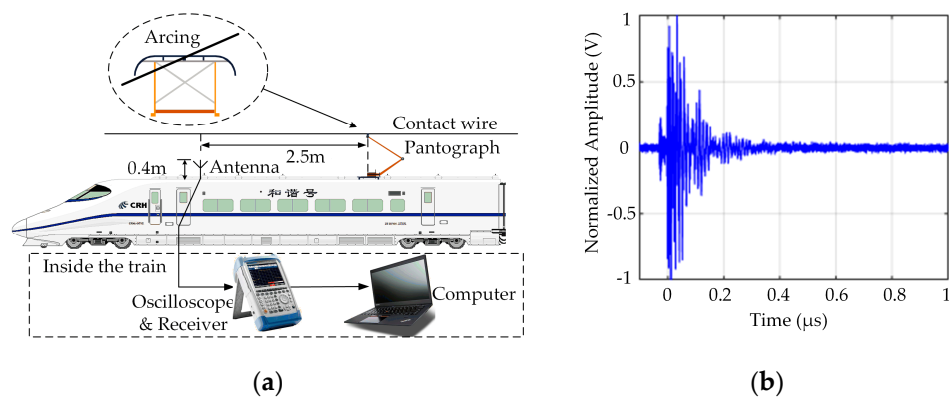

Figure 11. Measurement setup and results for A_{v2} of the node v_2. (**a**) Setup description of the on-site measurement in Chinese high-speed railway; (**b**) The result of the pantograph arcing.

2. $A_{e14\text{-}17}$ of the edge $e_{14\text{-}17}$

In general, there are two kinds of radiated parts from the structure including pantograph, contact wire, and train roof while the arc discharge happens. The primary direct radiation is from the arc itself and the other is the secondary radiation generated by the induced current in the pantograph and contact wire. Therefore, the signal in v_2 is the excitation of the structure of the pantograph-contact wire and the energy will be radiated by the equivalent antenna. Considering the large dimension in the longitudinal direction of the contact wire in a catenary, the equivalent antenna can be regarded as the Traveling Wave Wire Antenna. Thus, $A_{e14\text{-}17}$ of the edge $e_{14\text{-}17}$ can be represented by the model of the whole structure including pantograph, contact wire, and train roof in CST software as shown in Figure 12.
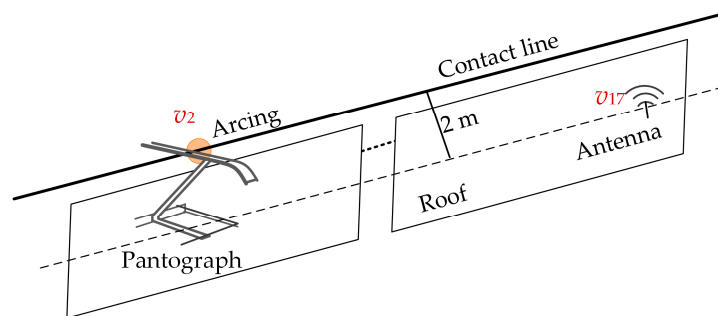

Figure 12. The attribute model of the edge $e_{14\text{-}17}$ by a simplified model for the connection between node v_2 and v_{17}.

In the model in Figure 12, the excitation is modeled as a discrete source between contact wire and pantograph with the continuous disturbance from v_2, and the gap between pantograph and contact line is built as 5 mm. v_{17} is the receiver at the end of the roof. In this model, the size of the train roof is set at 25 m × 4 m × 0.03 m with the material aluminum. Since the roof is the main reflective structure, the carriage is simplified and represented by the roof. The height of the contact line and the roof is set to 2 m. The vertical distance between the contact line and the roof is set at 2 m. Since the actual length of the contact line is much longer than the train, the load is added on the contact line terminals at a quarter-wavelength position to avoid the influence in the simulation.

Based on the above analysis, the node of v_{17} is simulated as a receiving probe corresponding to the function in OTCS. Thus, the path $v_2 \rightarrow v_{14} \rightarrow v_{17}$ that the propagation characteristics could be

analyzed according to the model above. Furthermore, the electric field at the v_{17} position could be obtained by this model. However, it is different from the real environment in the high-speed railway. To get the actual signal for the next segment in the path, the signal is measured at the node of v_{17} and the result is shown in Figure 13. The pulse received at the v_{17} position is in Figure 13a and it has the same trends in Figure 11b. The port voltage received at the antenna cable of the module node v_{26} is shown in Figure 13b. Thus, the analysis process indicates the feasibility of the path $v_2 \rightarrow v_{14} \rightarrow v_{17}$ in the EN model.
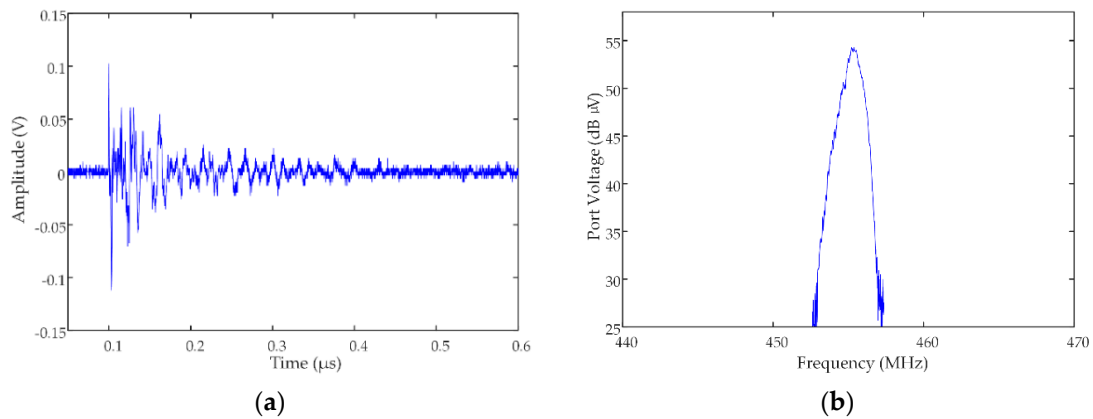

(a)　　　　　　　　　　　　　(b)

Figure 13. The results at node v_{17}. (**a**) The pulse received at the antenna position in the EMU (**b**) The port voltage received at the antenna cable of the module node v_{26}.

3.　A_{v26} of the node v_{26}

To complete the case analysis, a downlink of LTE-R is established in Matlab for evaluating the path $e_{17\text{-}26}$ as shown in Figure 14. Since the throughput is an important criterion for evaluating the communication system, the throughput, as a basic index, is chosen as the attribute A_{v26} of node v_{26}. Thus, the path $v_2 \rightarrow v_{14} \rightarrow v_{17} \rightarrow v_{26}$ could be complete after the study above.
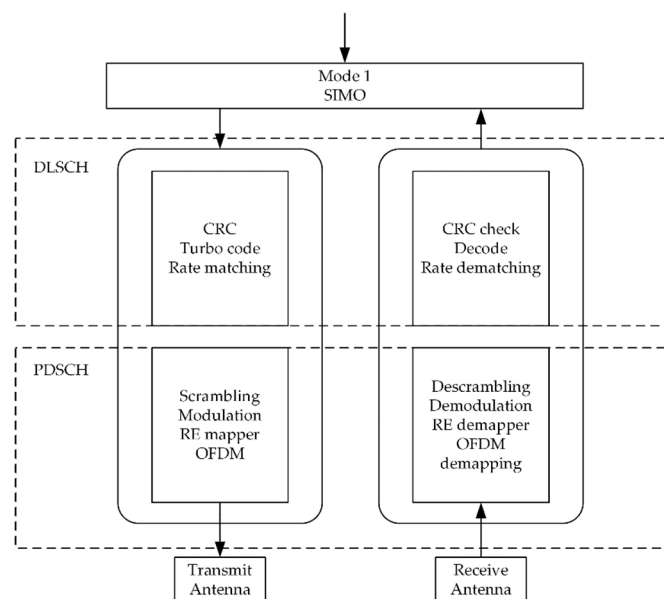

Figure 14. The structure of the downlink model.

In the downlink model of $e_{17\text{-}26}$, PDSCH (Physical Downlink Shared Channel) with modulation of 64QAM is selected for downlink simulation by the single antenna transceiver and the carrier frequency is 450 MHz with FDD standard [26]. The channel is AWGN and the bandwidth is 5 MHz. The port voltage received after the node v_{17} at the cable end in Figure 13b is added to the transmission channel. The relationship between the throughput and SNR (Signal to noise ratio) is shown in Figure 15 with the blue line. The throughput decreases when the disturbance caused by the pantograph arcing from the node v_2.
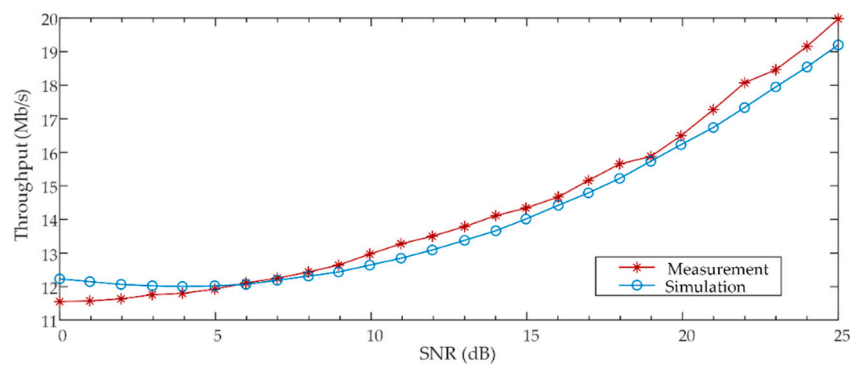

Figure 15. The evaluation criterion for Av26 of the node v26 with the relationship throughput and SNR.

In Figure 15, the measurement result is from the work in Reference [25]. It indicates the result is consistent with the simulation in $e_{17\text{-}26}$. It is based on the FTP (File Transfer Protocol) to measure the throughput of the LTE-R system in an experimental high-speed railway line in Shenyang, China. The on-board and wayside terminal will transfer a 100 MB file when the train passes through the coverage area of the network. Then, the device calculates the maximum number of bytes per second and we fit the relationship between the downlink throughput and the SNR.

The measurement results verify the validity of the simulation of the path $v_{17} \rightarrow v_{26}$. Thus, the EMI event of $v_2 \rightarrow v_{14} \rightarrow v_{17} \rightarrow v_{26}$ in the EN model of the OTCS has been analyzed and the results show that the pantograph arcing disturbance will affect the performance of communication.

4.3.2. Path B

1.　A_{v5} of the node v_5

As the description in Section 3.1.1, the conductive EM disturbances from the channel of "pantograph—traction transformer—converter—power line—ground device" will make the interactions between the power system and OTCS equipment. The factory workers may lay the cable between DMI device v_{15} and the OTCS kernel v_{20} at the installation space together with the power cables inside the train body for saving space. However, this condition leads to the EMI event in path B occurs.

The waveform in Figure 16 is selected as the attribute of A_{v5} as the equivalent conduction disturbance from the railway system by measurement [27]. The amplitude voltage of the actual measurement transient signal is about 5.3 V. Thus, the disturbance showed in Figure 16 with 2.5 µs duration is regarded as one signal in A_{v5}.
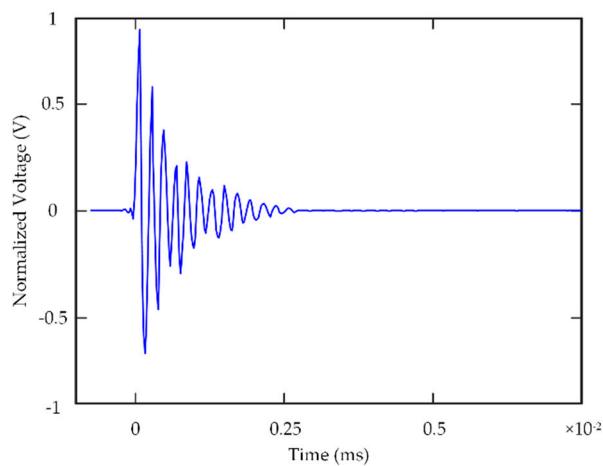
Figure 16. The waveform from the node v_5.

2. $A_{e13\text{-}16}$ of the edge $e_{13\text{-}16}$

According to the layout of the EMU, the power wire v_5 is a long cable with the 220 V, 50 Hz AC, and the resistance at both ends is 50 Ω. The DMI cable v_{16} is placed parallel to v_5. Therefore, the signal in v_5 is the source of the EMI path and the terminal at v_{20} will receive the disturbance signal. Considering the basic shape of the EMU, a rectangular body is used to simulate the train body. The size of the train is set at 25 m × 4 m × 4 m with 0.03 mm material aluminum in thickness. The DMI cable is close to the sidewall of the train body, 30 cm away from the ground and the sidewall. The power line and the DMI cable are routed in parallel, and the length is 20 m, as shown in Figure 17. Then, the core of the power cable is 0.75 mm^2, and the core of the DMI cable is 0.5 mm^2, and the shielding thickness of them is both 0.5 mm. The terminal v_{20} is connected to the 120 Ω load, and the terminal v_5 is connected to a load of 150 Ω.
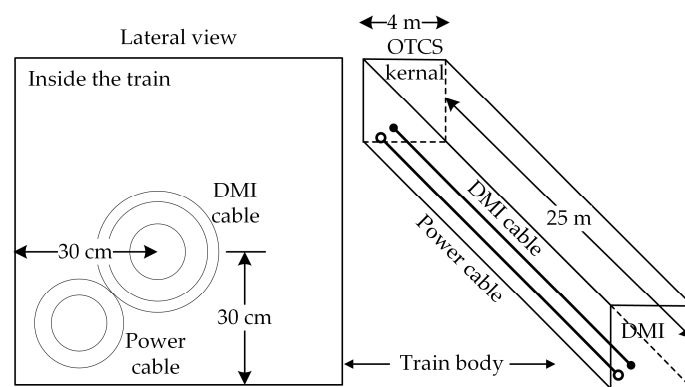

Figure 17. The attribute model of the edge $e_{13\text{-}16}$.

Based on the above analysis and configuration, the node v_{20} is simulated as the port signal at end of the cable v_{16} corresponding to the receiver function in OTCS. Then, the path $v_5 \rightarrow v_{16} \rightarrow v_{20}$ that the cable coupling EMI event could be analyzed according to the model above.

3. A_{v20} of the node v_{20}

In the first scene, it is assumed that the node v_{15} sends a square wave signal with the amplitude of 2.5 V, the duration is 0.07 ms, and the rising time is 1 μs. The result in Figure 18a is the ideal waveform, that is, there is no power cable nearby, the cable v_{16} is only influenced by the body and grounding current. The waveform in Figure 18b is the second scene where the power cable v_5 is placed next to the cable v_{16}. In Figure 18, it can be known that the cable coupling has affected the node v_{16},

however, the communication function between nodes v_{15} and v_{20} is still normal due to the low received disturbance level.
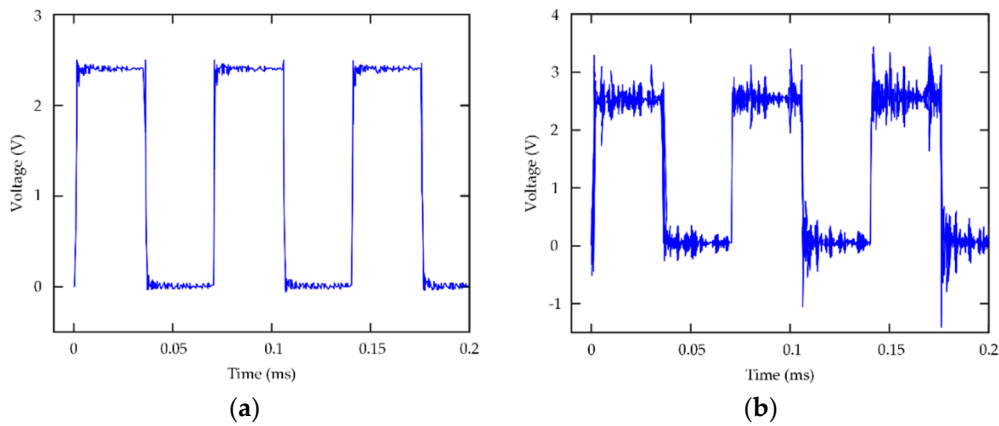

Figure 18. The results at node v_{20}. (**a**) No power cable near the DMI cable; (**b**) The signal received at the node v_{20} when the power cable is nearby.

In the second scene, the disturbance in Figure 17 is superimposed on the power cable with a 220 V AC signal, and the result at node v_{20} is shown in Figure 19a. The figure shows that the power cable has an impact on the signal of the DMI cable. Assuming that the transmission is the differential mode of RS485, thus, the difference between the two cores determines the terminal signal. It can be found in the figure that the voltage difference between cores has reached about 7 V, which obviously exceeds its normal decision level. Thus, it may cause the fault detailed in "communication interruption error".
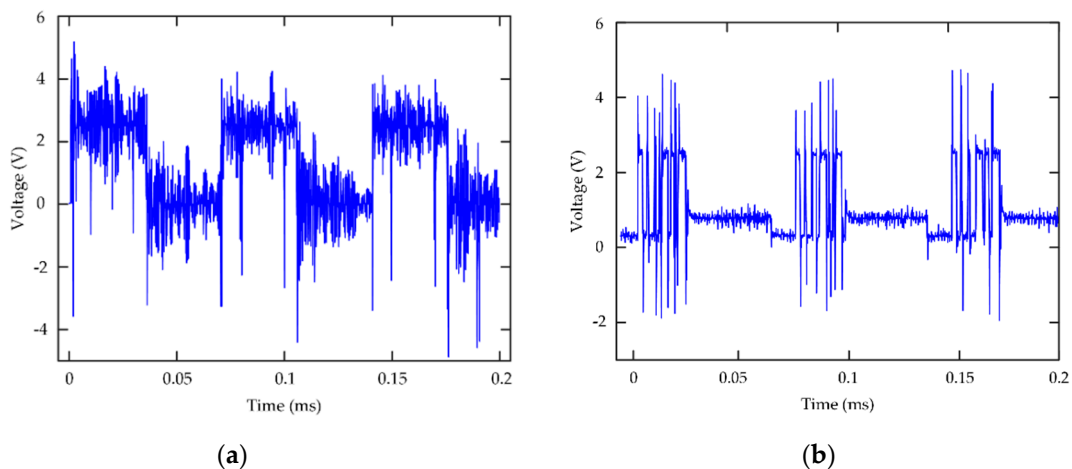

Figure 19. The results at node v_{20} with the disturbance. (**a**) The power cable with the disturbance source; (**b**) The signal measured at the port of node v_{20} in OTCS.

To verify the analysis results, the measure results in time-domain at the port of node v_{20} in OTCS is shown in Figure 19b. Taking into account the actual cable length, the amplitude of the disturbance and the protective measures, the waveform of the measured result is relatively smooth than the simulation. However, the amplitude received has reached the same level in Figure 19a, which exceeds the normal judgment amplitude.

The simulation and measurement results verify the validity of the path $v_5 \rightarrow v_{20}$. Thus, the EMI event of $v_5 \rightarrow v_{13} \rightarrow v_{16} \rightarrow v_{20}$ in the EN model of the OTCS has been analyzed and the results show that the disturbance from the traction system would affect the communication between v_{15} and v_{20} if the power cable is nearby.

5. Conclusions

This paper proposes a network-based modeling method for EMI event analysis in OTCS, which decomposes the OTCS and EMU into nodes and edges to abstractly present the elements of EMC and equipment, making EMC analysis in system-level view possible. By combining the EM sources, sensitive equipment, and coupling into different paths in the EN model, each EMI event can be studied from the origin node to the destination based on calculation, simulation, or measurement, respectively.

The modeling method based on network theory for EMI events under the high-speed railway EM environment is applied to the OTCS equipment in the EMU. The model has 26 nodes in this version with 9 disturbance nodes and 12 equipment nodes, respectively. The cases from the EMI event paths have been analyzed under the framework of the EN model, and the results indicate the new method is operable. Considering the analysis process, it is helpful for us to investigate EMI events and improve EMC performance in railway engineering. The modeling method describes the analysis process of the paths clearly and indicates the feasibility of the EN model. Besides, if all paths can be done like the cases and the new EMI event will be added in the updated model, a more integral model will be carried out to develop the EMC performance of the OTCS at the system-level in the future.

References

1. Pozzobon, P.; Amendolara, A.; Vittorini, B.; Henning, U.; Schmid, R.; Shirran, S.; Ahlstedt, S. Electromagnetic compatibility of advanced rail transport signalling. In Proceedings of the 2003 the World Congress on Railway Research, Edinburgh, UK, 28 September–1 October 2003.
2. Rodriguez, L.; Pinedo, C.; Lopez, I.; Aguado, M.; Astorga, J.; Higuero, M.; Adin, I.; Bistué, G.; Mendizabal, J. Eurobalise-Train communication modelling to assess interferences in railway control signalling systems. *Netw. Protoc. Algorithms* **2016**, *8*, 58. [CrossRef]
3. Huang, K.; Liu, Z.; Zhu, F.; Zheng, Z.; Cheng, Y. Evaluation Scheme for EMI of Train Body Voltage Fluctuation on the BCU Speed Sensor Measurement. *IEEE Trans. Instrum. Meas.* **2017**, *66*, 1046–1057. [CrossRef]
4. Midya, S.; Thottappillil, R. An overview of electromagnetic compatibility challenges in European Rail Traffic Management System. *Transp. Res. Part C Emerg. Technol.* **2008**, *16*, 515–534. [CrossRef]
5. Wu, Y.; Weng, J.; Tang, Z.; Li, X.; Deng, R.H. Vulnerabilities, Attacks, and Countermeasures in Balise-Based Train Control Systems. *IEEE Trans. Intell. Transp. Syst.* **2017**, *18*, 814–823. [CrossRef]
6. *Railway Applications—Electromagnetic Compatibility—Part 1–5*; IEC 62236—1-5:2018; IEC: Geneva, Switzerland, 2018.
7. Tellini, B.; Macucci, M.; Giannetti, R.; Antonacci, G.A. Conducted and radiated interference measurements in the line-pantograph system. *IEEE Trans. Instrum. Meas.* **2001**, *50*, 1661–1664. [CrossRef]
8. Midya, S.; Bormann, D.; Schutte, T.; Thottappillil, R. Pantograph Arcing in Electrified Railways—Mechanism and Influence of Various Parameters—Part II: With AC Traction Power Supply. *IEEE Trans. Power Deliv.* **2009**, *24*, 1940–1950. [CrossRef]
9. Ma, L.; Wen, Y.; Marvin, A.; Karadimou, E.; Armstrong, R.; Cao, H. A Novel Method for Calculating the Radiated Disturbance from Pantograph Arcing in High-Speed Railway. *IEEE Trans. Veh. Technol.* **2017**, *66*, 8734–8745. [CrossRef]
10. Bellan, D.; Spadacini, G.; Fedeli, E.; Pignari, S.A. Space-Frequency Analysis and Experimental Measurement of Magnetic Field Emissions Radiated by High-Speed Railway Systems. *IEEE Trans. Electromagn. Compat.* **2013**, *55*, 1031–1042. [CrossRef]
11. Hill, R.J. Electric railway traction. Part 7: Electromagnetic interference in traction systems. *Power Eng. J.* **1997**, *11*, 259–266. [CrossRef]

12. Hill, R.J. Electric railway traction. Part 6: Electromagnetic compatibility disturbance—Sources and equipment susceptibility. *Power Eng. J.* **1997**, *11*, 31–39. [CrossRef]

13. Jia, K. *High Frequency Model of Electrified Railway Propulsion System for EMC Analysis*; Kungliga Tekniska Högskolan: Stockholm, Sweden, 2012.

14. Pous, M.; Azpurua, M.A.; Silva, F. Measurement and Evaluation Techniques to Estimate the Degradation Produced by the Radiated Transients Interference to the GSM System. *IEEE Trans. Electromagn. Compat.* **2015**, *57*, 1382–1390. [CrossRef]

15. Dudoyer, S.; Deniau, V.; Adriano, R.R.; Slimen, M.N.B.; Rioult, J.J.; Meyniel, B.; Berbineau, M.M. Study of the Susceptibility of the GSM-R Communications Face to the Electromagnetic Interferences of the Rail Environment. *IEEE Trans. Electromagn. Compat.* **2012**, *54*, 667–676. [CrossRef]

16. Guo, Y.; Zhang, J. Analysis of Electromagnetic Compatibility of EMU Onboard BTM Equipment. *J. China Railw. Soc.* **2016**, *38*, 75–79.

17. Mariscotti, A.; Ruscelli, M.; Vanti, M. Modeling of Audiofrequency Track Circuits for Validation, Tuning, and Conducted Interference Prediction. *IEEE Trans. Intell. Transp. Syst.* **2010**, *11*, 52–60. [CrossRef]

18. Li, Z.; Zheng, S.; Xu, Z.; Zhao, Y. Analysis on the Coupling Disturbance of ZPW-2000A Jointless Track Circuit under High Speed Condition and Countermeasures. *China Railw. Sci.* **2010**, *31*, 99–106.

19. Zhang, D.; Wen, Y.; Zhang, J.; Xiao, J.; Liu, D.; Xin, G. Coupling Analysis for Shielded Cables in the Train Using Hybrid Method. *IEEE Access* **2019**, *7*, 76022–76029. [CrossRef]

20. Tesche, F.M.; Ianoz, M.; Karlsson, T. *EMC Analysis Methods and Computational Models*; Wiley: New York, NY, USA, 1997.

21. Baum, C.E. Electromagnetic Topology a Formal Approach to the Analysis and Design of Complex Electronic Systems. Interaction Notes 400. 1980. Available online: http://ece-research.unm.edu/summa/notes/In/0400.pdf (accessed on 14 November 2020).

22. Lin, S.; Wang, Y.; Jia, L.; Zhang, H. Reliability assessment of complex electromechanical systems: A network perspective. *Qual. Reliab. Eng. Int.* **2018**, *34*, 772–790. [CrossRef]

23. Zhang, Y.; Wang, H.; Yuan, T.; Lv, J.; Xu, T. Hybrid Online Safety Observer for CTCS-3 Train Control System On-Board Equipment. *IEEE Trans. Intell. Transp. Syst.* **2019**, *20*, 925–934. [CrossRef]

24. Li, K.; Yao, X.; Chen, D.; Yuan, L.; Zhou, D. HAZOP Study on the CTCS-3 Onboard System. *IEEE Trans. Intell. Transp. Syst.* **2015**, *16*, 162–171. [CrossRef]

25. Li, C. *Research on High Speed Adaptability of Railway LTE-R Broadband Mobile Communication System*; China Academy of Railway Science: Beijing, China, 2019.

26. Padaganur, S.K.; Mallapur, J.D. Performance analysis of PDSCH downlink & inter-cell interferece parameters in LTE network. In Proceedings of the 2018 2nd International Conference on Inventive Systems and Control (ICISC), Coimbatore, India, 19–20 January 2018; pp. 791–795.

27. Niska, S. *Measurements and Analysis of Electromagnetic Interferences in the Swedish Railway Systems*; Luleå University of Technology: Luleå, Sweden, 2008.